Applied Energy 88 (2011) 2305–2314

Contents lists available at ScienceDirect

Applied Energy

journal homepage: www.elsevier.com/locate/apenergy

Dual-injection: The flexible, bi-fuel concept for spark-ignition engines fuelled with various gasoline and biofuel blends

Xuesong Wu [a,b], Ritchie Daniel [b], Guohong Tian [b,c], Hongming Xu [b,*], Zuohua Huang [a], Dave Richardson [d]

[a] State Key Laboratory of Multiphase Flow in Power Engineering, Xi'an Jiaotong University, Xi'an, PR China
[b] The University of Birmingham, Birmingham B15 2TT, UK
[c] Sir Joseph Swan Centre, Newcastle University, Newcastle Upon Tyne NE1 7RU, UK
[d] Jaguar Advanced Powertrain Engineering, Jaguar Land Rover, UK

ARTICLE INFO

Article history:
Received 9 November 2010
Received in revised form 22 December 2010
Accepted 11 January 2011

Keywords:
Dual-injection
Bi-fuel
Biofuel
Cross-over theory
2,5-Dimethylfuran
Ethanol

ABSTRACT

Dual-injection strategies in spark-ignition engines allow the in-cylinder blending of two different fuels at any blend ratio, when simultaneously combining port fuel injection (PFI) and direct-injection (DI). Either fuel can be used as the main fuel, depending on the engine demand and the fuel availability. This paper presents the preliminary investigation of such a flexible, bi-fuel concept using a single cylinder spark-ignition research engine. Gasoline has been used as the PFI fuel, while various mass fractions of gasoline, ethanol and 2,5-dimethylfuran (DMF) have been used in DI. The control of the excess air ratio during the in-cylinder mixing of two different fuels was realized using the cross-over theory of the carbon monoxide and oxygen emissions concentrations. The dual-injection results showed how the volumetric air flow rate, total input energy and indicated mean effective pressure (IMEP) increases with deceasing PFI mass fraction, regardless of the DI fuel. The indicated efficiency increases when using any ethanol fraction in DI and results in higher combustion and fuel conversion efficiencies compared to gasoline. Increasing the DMF mass fraction in DI reduces the combustion duration more significantly than with increased fractions of ethanol or gasoline in DI. The hydrocarbon (HC), oxides of nitrogen (NO_x) and carbon dioxide (CO_2) emissions mostly reduce when using any gasoline or ethanol fraction in DI. When using DMF, the HC emissions reduce, but the NO_x and CO_2 emissions increase.

1. Introduction

Major recent developments in internal combustion technology have focused on engine efficiency improvements and emissions reduction [1]. This is driven by the potentially damaging effect of global warming and the depletion in the supply of fossil fuels. The short- to mid-term solution has been found with the use of biofuels. In Europe, the promotion of biofuels in transportation is encouraging the wider use of biomass. Current legislation requires EU member states to conform to a 10% minimum target on the use of alternative fuels (biofuels or other renewable fuels) in transportation by 2020 [2]. In the US, tax incentives have been used to promote the use of ethanol in gasoline [3], in order to replicate the success seen in Brazil [4]. Therefore, the onus is on the automotive sector to optimize the use of these alternative fuels with modern technologies, such as direct-injection (DI), turbo- or super-charging, variable valve timing (VVT) and dual- or split-injection strategies.

Although the majority of light-duty spark-ignition engines in the US are equipped with PFI systems [1], most new production engines are increasingly fitted with DI systems. Despite the increased complexity and cost, DI systems offer more accurate fuelling control. However, through the combination of these two injection technologies, it is possible to exploit their individual advantages, further reducing fuel consumption and engine-out emissions, whilst maintaining high performance. For instance, the PFI system can help to reduce warm-up times, especially during cold starts [5] and help to minimize the particulate matter emissions [6]. On the other hand, the DI system can help to lower the engine-out emissions at low load by stratifying the in-cylinder charge and help to improve wide-open throttle (WOT) performance and fuel efficiency because of the increased volumetric efficiency compared to PFI. Most importantly, however, the dual-injection strategy offers an alternative approach to using gasoline–biofuel blends. The fossil fuel can be injected using the PFI system, while the biofuel can be injected using DI. This will help to lower the in-cylinder temperature due to the charge-cooling effect of DI, which will raise the air flow rate and increase the engine knocking limit. Consequently, the lower temperature will lower the NO_x emissions. The increased knock suppression ability from high octane biofuels,

* Corresponding author.
E-mail address: h.m.xu@bham.ac.uk (H. Xu).

0306-2619/$ - see front matter Crown Copyright © 2011 Published by Elsevier Ltd. All rights reserved.
doi:10.1016/j.apenergy.2011.01.025

such as ethanol, will help to promote the use of higher compression ratios for further efficiency gains, lower emissions and higher power densities. Not only does this concept offer a new approach to using gasoline–biofuel blends, it requires only small modifications to modern DI spark-ignition engines in order to implement the additional PFI system.

Currently, ethanol is the most widely used liquid biofuel [7,8]. It is used as a neat engine fuel or in various blends with gasoline especially in Brazil [9,10]. However, 2,5-dimethylfuran (DMF) has become an attractive biofuel candidate since the improved production methods were developed [11–14]. DMF's advantages over ethanol, which include a higher energy density and insolubility in water [15], have promoted its awareness as a promising gasoline-alternative fuel. Until recently, the research about DMF has focused on its production methods and fundamental combustion characteristics [15–23]. The authors of this paper recently reported the engine combustion and emissions characteristics of DMF [24]. They compared the engine performance and emissions of DMF, gasoline and ethanol at fixed spark timing regardless of load in a direct-injection spark-ignition single cylinder research engine. This preliminary work was enhanced through further experiments under gasoline MBT ignition timing and fuel-specific ignition timing [25].

Normally, when using gasoline–biofuel blends, the biofuel is externally mixed with gasoline using a specified blending ratio. However, the dual-injection strategy offers greater flexibility when using biofuels because varying blending ratios can be used by separately injecting different quantities of two different fuels into the engine simultaneously. The mixing ratio of the alternative fuel and fossil fuel can be altered instantly according to the engine demand and in-vehicle fuel availability. Therefore, the dual-injection strategy offers an alternative approach to meeting stringent emissions targets and future biofuel legislation.

Recently, Cohn et al. examined the potential of ethanol (hydrous and anhydrous) boosted direct- and dual-injection engines to help cool the charge and suppress knock [26–28]. Their work uses relatively modest hardware modifications without the development of new automotive components. Ikoma et al. also investigated the combination of PFI and DI fuelling using a 3.5 L V6 gasoline engine (2GR-FSE) to improve full-load performance. Their work demonstrates improved engine performance (fuel economy and torque) and reduced emissions [29]. Furthermore, Ford's 'Ecoboost' gasoline turbo-charged direct-injection (GTDI) engine has been tested using the dual-injection strategy. Here, PFI gasoline and DI E85 (15% gasoline and 85% ethanol, by volume) was used to improve the engine efficiency and to avoid knock at high load [30]. Similarly, Ford's ongoing research engine -'Bobcat', will use the dual-injection strategy at higher compression ratios to achieve greater mechanical efficiencies [31]. Finally, Zhu and co-workers studied the combustion characteristics of a single cylinder engine equipped with a dual-injection strategy [32,33]. Their results showed that the indicated mean effective pressure (IMEP) decreases with increased DI fuelling, except for some instances when using gasoline PFI and E85 in DI.

This study presents the preliminary investigation into the combustion and emissions characteristics of a single cylinder, 4-stroke spark-ignition engine fuelled with gasoline, ethanol and DMF under the dual-injection strategy. The engine setup, experimental results and finally conclusions are discussed in the following sections.

2. Experimental setup

2.1. Engine and instrumentation

The dual-injection experiments were performed on a single cylinder, 4-stroke spark-ignition research engine, as shown in Fig. 1. The engine specification is shown in Table 1. The engine is equipped with both high pressure (15 MPa) spray-guided DI and low pressure (0.3 MPa) PFI systems. The two fuelling modes can be used separately or simultaneously.

The engine was coupled to a DC dynamometer to maintain a constant speed of 1500 rpm (±1 rpm) regardless of the engine torque output. The in-cylinder pressure was measured using a Kistler 6041A water-cooled pressure transducer. Coolant and oil temperatures were controlled to 358 K and 368 K (±3 K) respectively, using a Proportional Integral Differential (PID) controller. All temperatures were measured with K-type thermocouples. A 100 L intake buffer tank (approximately 200 times the engine's swept volume)

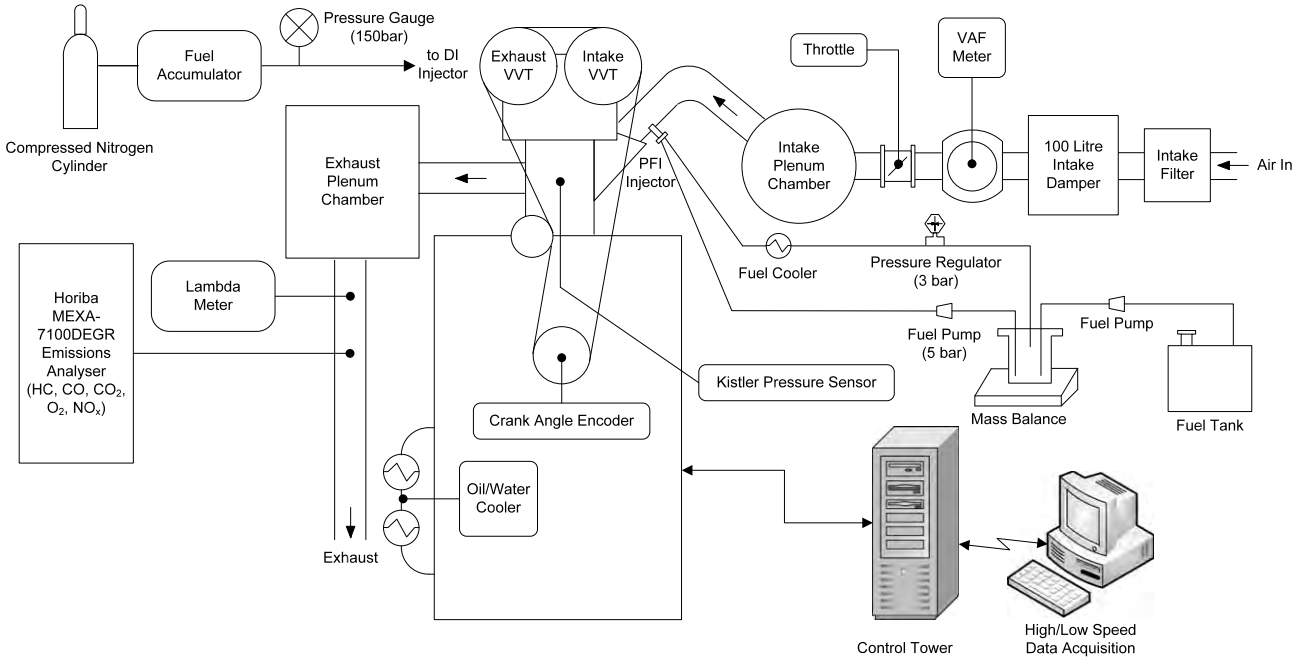

Fig. 1. Schematic of engine and instrumentation setup.

Table 1
Engine specification.

Engine type	4-stroke, 4-valve
Combustion system	Dual-injection: PFI and spray-guided DI SI
Swept volume	565.6 cm^3
Bore × stroke	90 × 88.9 mm
Compression ratio	11.5:1
Engine speed	1500 rpm
PFI pressure and timing	0.3 MPa, 50° bTDC
DI pressure and timing	15 MPa, 280° bTDC
Intake valve opening	16° bTDC
Exhaust valve closing	36° aTDC

was used to stabilize the intake air flow. The excess air ratio (λ) was controlled using the cross-over theory described in Section 2.4.

The engine was controlled using in-house control software written in LabVIEW. High-speed, crank-angle-resolved and low-speed, time-resolved data was also acquired using in-house LabVIEW program. This data was then analyzed using MATLAB to examine the combustion and emissions performance.

The gaseous emissions were measured using a Horiba MEXA-7100DEGR gas analyzer. Exhaust samples were taken 0.3 m downstream of the exhaust valve and pumped via a heated line (maintained at 464 K) to the analyzer.

2.2. Test fuels

In this study, three different fuels were used. The fuel properties are shown in Table 2. Both the gasoline and ethanol used in this study were supplied by Shell Global Solutions, UK. A high octane gasoline was chosen as this represents the most favorable characteristics offered by the market and provides a strong benchmark to the two biofuels. The DMF used in this study was supplied by Beijing LYS Chemicals Co Ltd. in China at 99.8% purity.

2.3. Experimental procedure

The engine was warm once the coolant and lubricating temperatures had stabilized at 358 K and 368 K respectively. All the tests were carried out at ambient air intake conditions (approximately 298 K) and the excess air ratio was controlled using the method described in the next section. For each test, the pressure data from 300 consecutive cycles was recorded and then averaged.

Each engine test began using 100% PFI gasoline for the desired initial intake manifold absolute pressures (MAP_i) of 0.065, 0.08 and 0.095 MPa at $\lambda = 1$, which represent low (0.45 MPa IMEP), medium (0.65 MPa IMEP) and high (0.85 MPa IMEP) initial engine loads when fuelled with gasoline, respectively. Such predetermined engine operating conditions were used to eliminate any engine effects and allow the comparison of the combustion and emissions performance between the three fuels to be made. Once stable, the PFI fuelling was gradually decreased until the desired injection duration was reached, which was based on the PFI injector calibration. Simultaneously, DI injection (gasoline, DMF or ethanol) was introduced, and was increased as necessary to maintain the required excess air ratio at the same throttle position and MAP_i. The target PFI mass fractions were: 100, 85, 70, 55, 40 and 0 of the 100% PFI case. At the lowest MAP_i (0.065 MPa), the required injection duration for the 40% PFI case was lower than the minimum opening time of the PFI injector and so was not recorded.

Throughout this study, gasoline was used as the PFI fuel, while the DI fuel was changed from gasoline to ethanol and then to DMF. Table 3 shows the test matrix. In this study, the spark timing was fixed at the knock-limited maximum brake torque (KL-MBT) timing of gasoline in PFI mode (25°, 13° and 7° CA bTDC for MAP_i of 0.065, 0.08 and 0.095 MPa respectively). The KL-MBT timing of gasoline was chosen in order to minimize the effect of spark timing on the engine combustion and emissions between fuels and avoid the knock phenomena because gasoline has the most retarded MBT or KL-MBT timing [25]. The injection timing of the DI fuel injection was also constant at 280° CA bTDC to achieve a homogenous mixture. To reduce experimental uncertainty, the same experiments were repeated three times and an average was taken. Error bars were then used to show the repeatability of this work.

Table 2
Test fuel properties.

	DMF	Ethanol	Gasoline
Chemical formula	C_6H_8O	C_2H_6O	C_2–C_{14}
H/C ratio	1.333	3	1.795
O/C ratio	0.167	0.5	0
Gravimetric oxygen content (%)	16.67	34.78	0
Density @ 20 °C (kg/m^3)	889.7*	790.9*	744.6
Research Octane Number (RON)	n/a	106	96.8
Stoichiometric air fuel ratio	10.72	8.95	14.46
LHV (MJ/kg)	32.89*	26.9*	42.9
LHV (MJ/L)	30*	21.3*	31.9
LHV of stoichiometric mixture (MJ/kg)	2.87	2.70	2.77
Heat of vaporization (kJ/kg)	332	840	373
Initial boiling point (°C)	92	78.4	32.8

* Measured using calorimeter system IKA C 200 at the University of Birmingham.

2.4. Excess air ratio control

As previously mentioned, the dual-injection tests were performed at stoichiometry. Conventionally in research, the air–fuel ratio (AFR) of a known fuel composition is measured using an appropriate lambda meter and oxygen sensor, which requires presetting the stoichiometric AFR value for either neat fuels or known fuel blends. However, in this study, the exact mixing ratio between the two fuels varies. Therefore, the authors have used the cross-over theory of the oxygen and carbon monoxide emissions concentrations, instead of the lambda meter and oxygen sensor combination, to control the excess air ratio.

The cross-over theory is not new, and is described in comprehensive engine textbooks [34,35]. It is based on the theory that close to stoichiometry, the oxygen (O_2) and carbon monoxide (CO) emissions concentrations are equal. When the mixture is lean, excessive air helps to oxidize the CO. Conversely, as the mixture becomes rich in fuel, the O_2 content decreases and the CO production increases inversely. Therefore, in the event of an AFR sweep, the O_2 and CO emissions can be shown by two separate curves which cross-over close to stoichiometry. This cross-over phenomenon provides another approach in controlling the in-cylinder AFR. However, there is no readily available information which confirms this phenomenon using oxygen content fuels like ethanol or DMF in pure or blended forms with gasoline. Therefore, the authors conducted a series of experiments to verify this technique for oxygen content fuels.

Firstly, four pure fuels and two fuel blends were chosen to confirm the cross-over theory under an arbitrary medium load of 0.65 MPa IMEP using 100% DI fuelling. For the excess air ratio sweep test, the excess air ratio was incrementally adjusted from

Table 3
Test matrix.

MAP_i (MPa)	Spark timing (°CA bTDC)	$PFI_x/PFI_{100\%}$ (%)
0.065	25	100, 85, 70, 55, 0
0.08	13	100, 85, 70, 55, 40, 0
0.095	7	100, 85, 70, 55, 40, 0

0.8 to 1.2 in steps of 0.05. The excess air ratio of these known fuel compositions was measured by the ETAS LA4 lambda meter and the Bosch heated LSU wideband lambda sensor. The throttle position was held constant throughout the test (equal to the 0.65 MPa IMEP, $\lambda = 1$ case). The injection duration was changed in order to match the required excess air ratio whilst maintaining the same throttle position. The gaseous emissions were recorded using the Horiba emissions analyzer once the engine was stable. The average results of the three repeats are shown in Fig. 2. It is clear that the cross-over excess air ratio remains close to stoichiometry, with a maximum absolute deviation between all six fuels less than 1%. This, therefore, validates the cross-over theory with high accuracy at 0.65 MPa IMEP using 100% DI. However, in order to verify this theory at different loads, further experiments using a wider load range were carried out. This time, the engine was run at low, medium and high loads (0.45, 0.65 and 0.85 MPa IMEP) at the measured cross-over locations of the O_2 and CO concentrations, using the Horiba emissions analyzer. Fig. 3 compiles the corresponding excess air ratios at their respective cross-over points for the three engine loads. For the six different fuels, the deviation from stoichiometry is less than 1% at 0.45 and 0.65 MPa IMEP. However, for 0.85 MPa IMEP, the cross-over excess air ratio is slightly lean, between 1.005 and 1.03. Nevertheless, this is less than 3% of stoichiometry and the error is within acceptable experimental uncertainty (95% confidence level).

Therefore, it is believed that the cross-over theory can be used to control the excess air ratio for the in-cylinder mixing of different fuels to high accuracy. Although the mixture is slightly lean at the highest load (0.85 MPa IMEP), this method is acceptable if it is consistently applied to all fuel combinations.

3. Results and discussion

The results in this section are shown using stacked graphs to reflect the three initial conditions (MAP_i). For each normalized graph, the vertical axis shows the relative change in each key parameter from the 100% PFI condition. The horizontal axis shows the reduction in the PFI mass fraction, also from the 100% PFI condition, which has been compensated for using DI fuelling to maintain stoichiometry. Each fuel has been shown using different line types, colors and symbols (solid green lines with circle markers for gasoline, short dashed red lines with triangle markers for DMF and dashed dot blue lines with square markers for ethanol). Error bars have been used to highlight the test repeatability.

3.1. Volumetric air flow rate

Fig. 4 shows the relationship between the normalized volumetric air flow rate to the 100% PFI condition and the PFI mass fraction for the three fuels at the three MAP_i. The volumetric air flow rate increases with decreasing PFI mass fraction regardless of the MAP_i and the DI fuel used. This is largely due to the effects of charge-cooling and PFI partial pressure. The effect of charge-cooling helps to lower the in-cylinder charge temperature and increase the volumetric efficiency [36], whilst further suppressing knock. For gasoline, the maximum increase in volumetric air flow rate at the MAP_i of 0.065 MPa is 1.1%. The vaporization of the gasoline causes the intake air to cool, which increases its density and thus allows more air to flow into the cylinder. Meanwhile, the partial pressure of the PFI fuel will decrease with decreasing PFI mass fraction, which also improves the volumetric air flow rate. The increase in volumetric air flow rate for ethanol is much higher than that for gasoline and DMF, regardless of the MAP_i. This is caused by two reasons. Firstly, ethanol has a much higher latent heat of vaporization, which results in more charge-cooling (see Table 2). Secondly, ethanol has a lower stoichiometric AFR, so, in order to maintain a stoichiometric mixture, more ethanol is required, which amplifies the aforementioned increased charge-cooling effect. For DMF, the heat of vaporization is marginally lower than that for gasoline (see Table 2). Although this would help with engine cold starts, it produces less cooling when the engine is warm. However, DMF has a lower stoichiometric AFR compared to gasoline, which requires more fuel at the same MAP_i. Therefore, the combined effects of the latent heat of vaporization and the stoichiometric AFR make the volumetric air flow rate of DMF fuelling comparative to that of gasoline. As shown in Fig. 4, the volumetric air flow rate when using gasoline in DI is, in most cases, very close to that for DMF. Nevertheless, the improvement with volumetric air flow rate is seen throughout the dual-injection strategy and so offers benefits over the 100% PFI case.

3.2. Total input energy and engine load

Fig. 5 shows the variation of normalized total input energy with reducing PFI mass fraction for the three fuels at the three different MAP_i. For gasoline, the total input energy slightly increases with the decrease of the PFI mass fraction at each MAP_i. This is due to the increase of the volumetric air flow rate as explained previously. For ethanol and DMF, the total input energy also increases. As

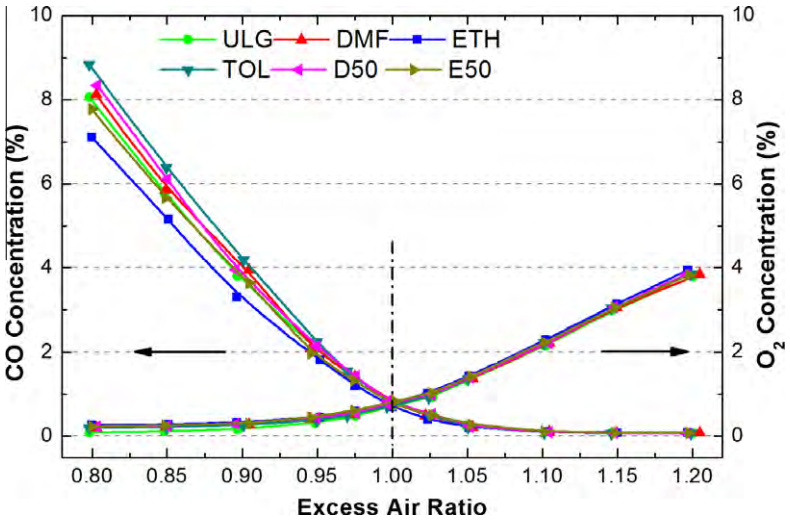

Fig. 2. Oxygen and carbon monoxide concentration with varying excess air ratio at 0.65 MPa IMEP in DI mode only using four pure Fuels and two fuel blends.

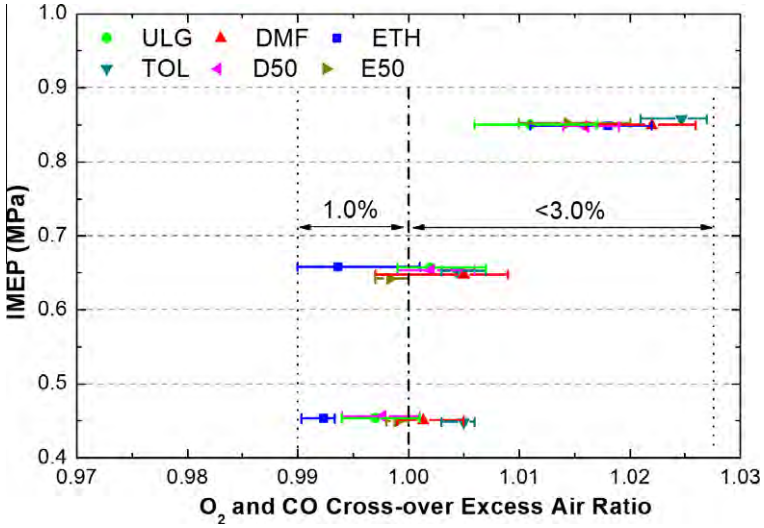

Fig. 3. Oxygen and carbon monoxide cross-over excess air ratio with varying load in DI mode only using four pure fuels and two fuel blends.

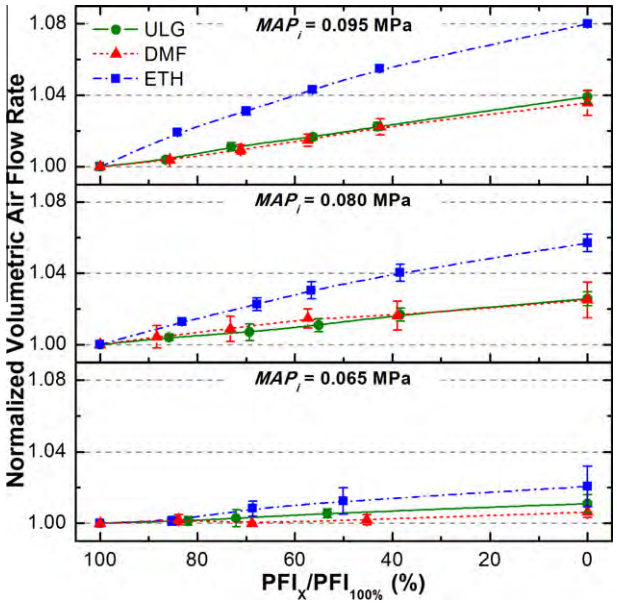

Fig. 4. Normalized volumetric air flow rate to 100% PFI condition with reduced mass fractions of PFI fuelling using gasoline, DMF and ethanol at three different MAP_i.

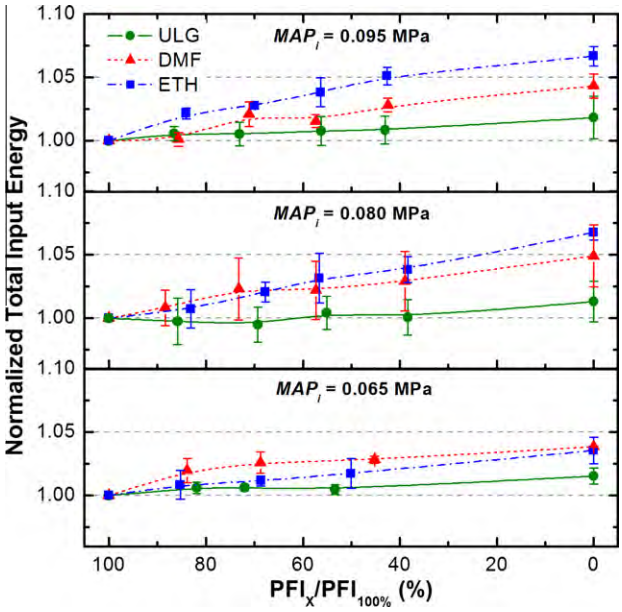

Fig. 5. Normalized total energy to 100% PFI condition with reduced mass fractions of PFI fuelling using gasoline, DMF and ethanol at three different MAP_i.

shown in Table 2, the stoichiometric AFR and lower heating value (LHV) decrease in the order of gasoline, DMF and then ethanol. However, this does not necessarily result in a similar order of decrease for total input energy. Although DMF and ethanol would need more fuel for the same intake volumetric air flow rate and stoichiometric mixture in an adiabatic process, the charge-cooling effect, which is much more prominent for ethanol, alters the intake conditions. As mentioned, the volumetric air flow rate when using increased ethanol in DI, increases more so than with gasoline (shown in Fig. 4). This increases the total input energy delivered by ethanol in DI in order to maintain stoichiometry. As shown in Fig. 5, the total input energy of ethanol and DMF is higher than that of gasoline, regardless of the MAP_i. This is due to the combined effects of the quantities of the injected fuel and their LHV. At the lowest MAP_i, the total input energy when using increased mass fractions of DMF in DI is slightly higher than that when using ethanol. However, as the MAP_i is increased, the total input energy required when using ethanol now surpasses that when using DMF. This is largely because of the greater charge-cooling effect of ethanol as shown by Fig. 4. This increase in input energy provides a greater opportunity for higher power outputs. Therefore, the relationship with the reduced PFI mass fraction and fuel is shown in Fig. 6. The IMEP when using increased fractions of ethanol in DI exceeds that with gasoline and DMF.

Fig. 6 shows the relationship between the normalized IMEP and the PFI mass fraction for the three fuels at the three different MAP_i. For all three fuels, the IMEP increases with the decrease of the PFI mass fraction. This is largely due to the effect of the increasing total input energy. The increase in IMEP when using DMF in DI is larger than that with gasoline. Although the increase in the total input energy for ethanol is not the highest at the low MAP_i, the increase of the IMEP for ethanol is the highest amongst the three fuels at each MAP_i. This demonstrates a higher indicated efficiency of ethanol compared to DMF and gasoline: less input energy is required to give greater output energy. As the MAP_i increases, the near-lin-

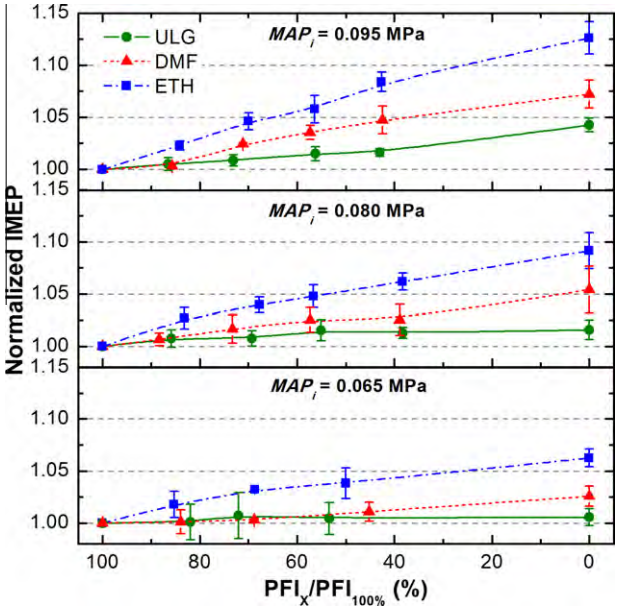

Fig. 6. Normalized IMEP to 100% PFI condition with reduced mass fractions of PFI fuelling using gasoline, DMF and ethanol at three different MAP_i.

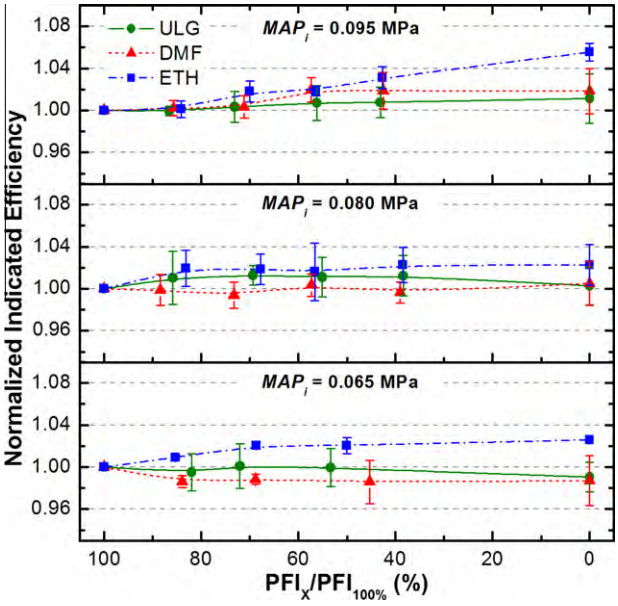

Fig. 7. Normalized indicated efficiency to 100% PFI condition with reduced mass fractions of PFI using gasoline, DMF and ethanol at three different MAP_i.

ear rate of IMEP increase from 100% PFI to 0% PFI also increases. With respect to the dual-injection strategy, greater benefits are found at higher MAP_i. At 0.065 MPa MAP_i, the performance benefits of increased DI fuelling using DMF over gasoline are unapparent. However, the benefits of the dual-injection strategy with ethanol are much more apparent even at 0.065 MPa MAP_i. Immediately, as the amount of PFI fuelling is reduced, the IMEP increase with ethanol is substantially higher than the equivalent PFI fuelling reduction when using gasoline and DMF in DI.

3.3. Efficiency

Fig. 7 shows the relationship between the normalized indicated efficiency and the PFI mass fraction for the three fuels at the three MAP_i. Throughout the present experimental conditions, ethanol in DI results in the highest normalized indicated efficiency. This is apparent from as low as approximately 85% PFI mass fraction (although not so obvious at 0.095 MPa MAP_i). This may be due to higher combustion and fuel conversion efficiencies (as shown in [25]) and the higher charge-cooling effect of ethanol compared to gasoline and DMF (see Fig. 4). At the two lowest MAP_i, DMF, on the other hand, is marginally less efficient than gasoline at converting the fuel energy into useful work. This may be due to the suboptimal spark timing despite having a greater resistance to knock. At the highest MAP_i, the indicated efficiency of increased DMF mass fractions in DI is higher than that when using gasoline. However, the difference is insignificant and within the error limits shown in Fig. 7. Previous studies by the authors have shown the normalized indicated specific gasoline equivalent fuel consumption (ISFCE) of ethanol and DMF, which is a measure of the fuel conversion efficiency and similar to the indicated efficiency, can be further improved by using the fuel specific KL-MBT timing, especially at the medium and high load [25]. Thus, further improvements are likely to be made to the indicated efficiency for ethanol and DMF through optimization on the parameters such as the timing of ignition and intake/exhaust valves.

3.4. In-cylinder pressure and combustion duration

Fig. 8 shows the crank-angle-derived pressure trace and corresponding heat release rate curves for the three fuels at the highest MAP_i (0.095 MPa MAP_i and 0.85 MPa load) and fixed ignition timing of 7° CA bTDC. For each fuel, the pressure traces for the 100%, 55% and 0% PFI mass fractions are compared. It clearly shows that the reduced PFI mass fractions result in higher and slightly earlier peak in-cylinder pressures (P_{max} and θ_{max} respectively). This behavior is emphasized when using DMF and ethanol. From previous work, it has been found that DMF has a faster combustion speed than gasoline possibly due to higher in-cylinder temperatures [25]. Therefore, when DMF fuel is introduced by the DI system (55% PFI case), the combustion duration reduces more so than with ethanol. This advances the location of θ_{max}. This is seen clearly at the 0% PFI condition. This reduction in combustion duration is shown in Fig. 9.

Fig. 8 also shows the heat release rate for three different fuels with different mass fractions in PFI at the MAP_i of 0.095 MPa. For all three fuels, the initial stage of heat release rate is unaffected by the dual-injection strategy. However, the later stages of heat release rate are influenced by decreasing PFI mass fractions. For gasoline, the heat release rate is marginally affected by decreased PFI fuelling. For 100% DI fuelling, the heat release rate peaks slightly earlier and higher compared to 100% PFI fuelling case. When using DMF, the higher in-cylinder temperature [25] and marginally faster laminar burning velocity [37] lead to higher and slightly earlier peak in heat release rate compared to gasoline. Similarly, when using ethanol, the heat release rate increases more quickly and peaks higher with decreasing PFI fuelling. So, in summary, the effect of decreasing the PFI mass fraction is an enhancement of the heat release and shortening the combustion duration at the MAP_i of 0.095 MPa for both DMF and ethanol.

Fig. 9 shows the relationship between the combustion duration (10–90% MFB) and the PFI mass fraction under the different MAP_i for the three fuels. The normalized combustion durations have a clear relationship with MAP_i. For gasoline, the normalized combustion duration increases as the PFI mass fraction is reduced, but the rate of this increase reduces as the MAP_i increases. Through optimization of the spark timing, the normalized combustion durations would be further reduced, due to the greater knock suppression quality of DI and the octane ratings of each fuel, as seen in [25]. For the three fuels, it is DMF that results in the lowest normalized combustion durations. This fast burning ability has also been seen

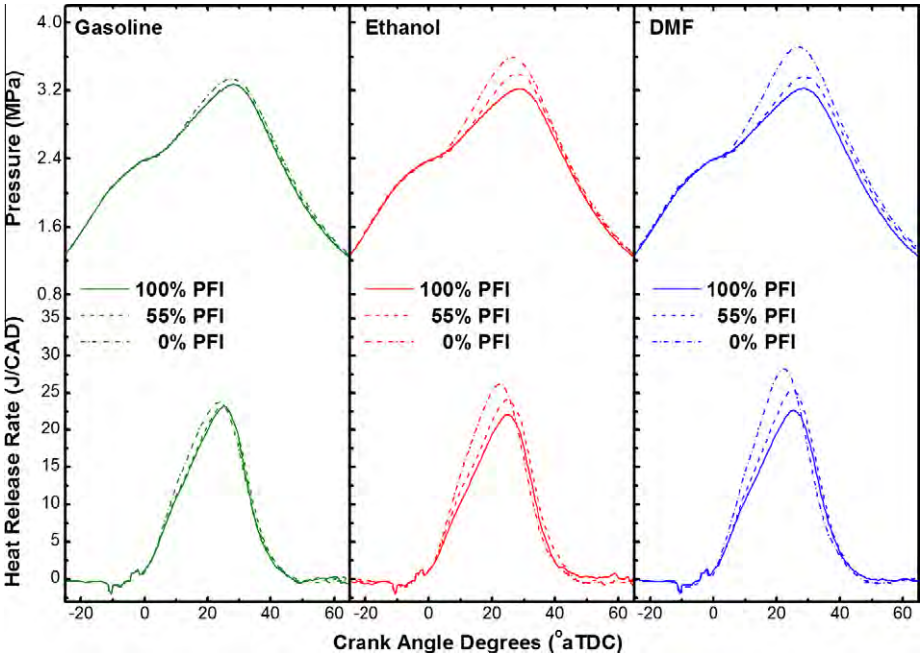

Fig. 8. In-cylinder pressure and heat release rate curves at the MAP_i of 0.095 MPa with different fractions of PFI fuelling using gasoline, DMF and ethanol.

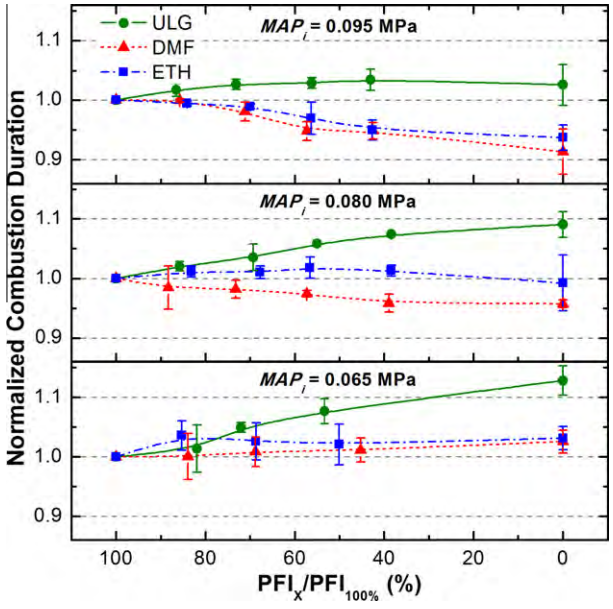

Fig. 9. Normalized combustion duration to 100% PFI condition with reduced mass fractions of PFI fuelling using gasoline, DMF and ethanol at three different MAP_i.

in previous engine work [24,25] despite DMF having a lower laminar flame velocity than ethanol [37]. This is believed to be due to higher combustion temperatures. Normally, shorter combustion durations result in higher efficiency. However, DMF does not satisfy this trend when compared to gasoline and ethanol at the two lowest MAP_i. As shown in Fig. 7, DMF has the lowest indicated efficiency at the two lowest MAP_i, but the efficiency difference between gasoline and DMF is small and within the error limits. This is perhaps because the combustion temperature of DMF is higher which results in more heat loss and lower useful work transfer [25]. However, at the highest MAP_i, the shorter combustion duration helps to increase the efficiency of DMF above that of gasoline (see Fig. 7). For ethanol, the combustion duration increases with the decrease of the PFI fraction at 0.08 MPa MAP_i, except at the 0% PFI case. In comparison, the combustion duration when using DMF decreases. This difference is due to lower combustion temperatures when using ethanol due to the higher charge-cooling effect. However, at the highest MAP_i, the combustion duration when using ethanol decreases with the decrease of the PFI mass fraction. As shown in Fig. 6, the IMEP significantly increases at the highest MAP_i resulting in even higher in-cylinder temperatures and pressures [25] which will further reduce the combustion duration.

3.5. Emissions

Fig. 10 shows the normalized indicated specific hydrocarbon emissions (ISHC). When using gasoline in DI, the ISHC emissions marginally increase at 0.065 MPa MAP_i as the PFI mass fraction is decreased. However, as the MAP_i is increased, the effect of gasoline in DI reduces the ISHC emissions. The ability of DI to lower the HC emissions is well proved [36]. This is largely due to the higher injection pressure, which improves liquid fuel atomization and reduces wall wetting. The ISHC emissions also reduce more greatly at the highest MAP_i due to the more prominent increase of load. Previous work has shown the ISHC emissions to decrease slightly with load [25,35], because the oxidation rate of the hydrogen and carbon molecules is improved. When using ethanol and DMF, the decrease of the PFI mass fractions reduces the ISHC emissions, regardless of the MAP_i. Both fuels contain an oxygen atom in their molecular structures, which helps to reduce the ISHC emissions as the oxygen is more readily available [38]. The higher relative increase in IMEP (Fig. 6), together with the more readily available oxygen atoms, improves the oxidation rate of the unburned hydrocarbons [35].

Fig. 11 shows the trend in the normalized indicated specific NO_x ($ISNO_x$) emissions between the three fuels. The NO_x emissions are related to the fuel type [38,39]. For the same excess air ratio, the nitric oxide or NO emissions, which represent the majority of NO_x emissions [35], decrease with increasing H:C ratio [39]. As shown in Table 2, the H:C ratio increases in the order of DMF, gas-

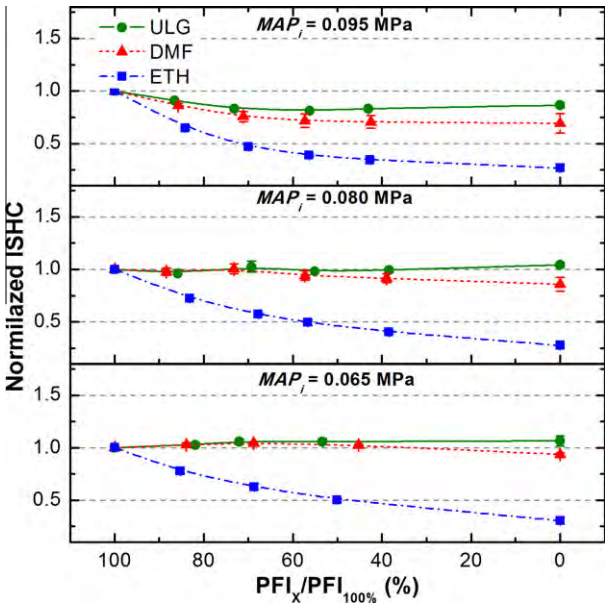

Fig. 10. Normalized indicated specific hydrocarbon emissions to 100% PFI condition with reduced mass fractions of PFI fuelling using gasoline, DMF and ethanol at three different MAP_i.

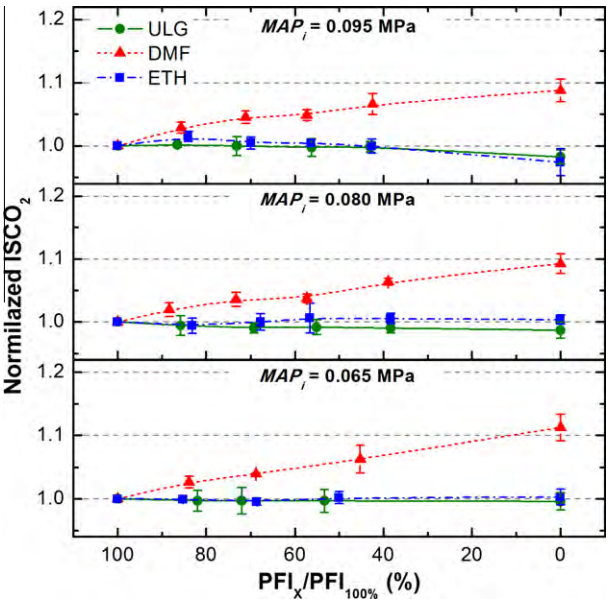

Fig. 12. Normalized indicated Specific carbon dioxide emissions to 100% PFI condition with reduced mass fractions of PFI fuelling using gasoline, DMF and ethanol at three different MAP_i.

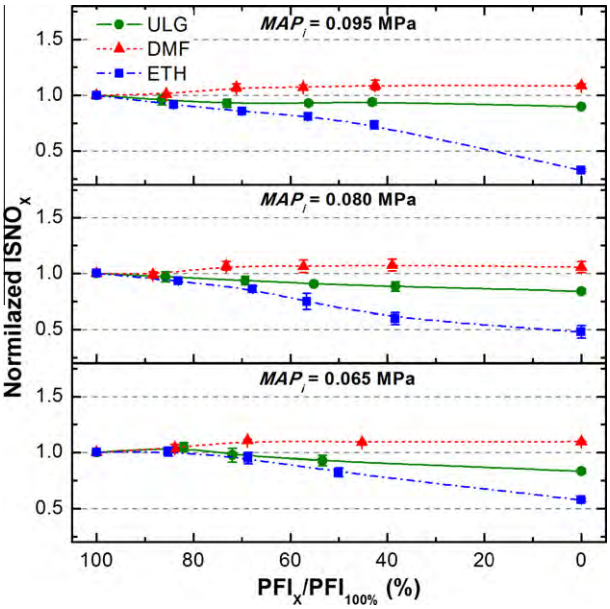

Fig. 11. Normalized indicated specific NO_x emissions to 100% PFI condition with reduced mass fractions of PFI fuelling using Gasoline, DMF and Ethanol at three different MAP_i.

oline, and then ethanol. Thus, the NO_x emissions should reflect this order based on the results shown in [39]. As shown in Fig. 11, the $ISNO_x$ emissions are in the decreasing order of DMF, gasoline, and ethanol which reflects the H:C ratio order. As previously mentioned, when reducing the PFI fuelling and thus increasing the DI fuelling, the charge-cooling effect is increased, which decreases the in-cylinder temperature and reduces the formation of NO_x. This effect is clearly shown with gasoline when switching from PFI to DI. As shown in Fig. 11, the $ISNO_x$ emissions decrease with decreasing PFI mass fraction when using ethanol and gasoline at each MAP_i, while increasing when using DMF. Although this decrease is moderate for gasoline, it is much more obvious for ethanol. Ethanol has a higher heat of vaporization and lower stoichimetric AFRs. Thus, the charge-cooling effect is much more prominent when using ethanol compared to gasoline. The increase in $ISNO_x$ for DMF may be due to the increase of the in-cylinder temperature as reported in previous work by the authors [24,25]. They found that DMF has the highest in-cylinder temperature compared to gasoline and ethanol.

Fig. 12 shows the normalized indicated specific carbon dioxide ($ISCO_2$) emissions. Carbon dioxide is a non-toxic gas and is not classified as a pollutant engine emission. However, in recent years, the monitoring of CO_2 emissions has become more critical because it is considered to contribute to global temperature rises. Thus, the normalized $ISCO_2$ emissions are shown in this work. For gasoline, the dual-injection strategy helps to reduce the $ISCO_2$ emissions at each MAP_i. The CO_2 emissions give an indication of the combustion efficiency and have been shown to decrease when switching from PFI to DI [5]. The drop in efficiency helps to explain the reduction in $ISCO_2$ emissions when using only gasoline. The H:C ratio also affects the CO_2 emissions concentration [35]. Previous work by the authors using gasoline optimized spark timing, showed that the $ISCO_2$ emissions for gasoline, ethanol and DMF all increased at high engine loads (>0.65 MPa) [25]. Therefore, although ethanol has the highest H:C ratio, which helps to reduce the $ISCO_2$ emissions, the relatively larger increase in IMEP compromises this benefit. This explains the similar $ISCO_2$ performance of ethanol and gasoline. When using DMF in DI, the $ISCO_2$ emissions increase at each MAP_i. This increase is mainly due to the lower H:C ratio. However, as a biofuel candidate, the lifecycle CO_2 emissions for DMF must be considered. DMF consumes CO_2 in its production stage, which would help to offset the increase in the engine-out CO_2 emissions.

4. Discussion

As shown, the dual-injection strategy shows advantages in engine performance and emissions over the 100% PFI case under the preset experimental conditions. However, the 100% DI case (0% PFI) still represents the most favored conditions. This raises

the debate over the relevance of the dual-injection strategy when the DI strategy is the most beneficial. There are two main attractions for the dual-injection strategy. Firstly, the dual-injection strategy offers an alternative approach to the external blending of biofuels with gasoline and promotes the use of in-cylinder blending in real-time. Secondly, it is well known that the PM emissions when using PFI are much lower than with DI [6]. Therefore, the dual-injection strategy can help to lower the PM emissions normally found with PFI whilst maintaining the competitive power output associated with DI. Although the dual-injection system would increase the hardware cost slightly compared with the DI engine, the engine operating modes will be more flexible and comply with increasing biofuel obligation.

After all, the experimental data in this study were collected under the condition of fixed ignition, injection and valve timings. Therefore, in order to further assess the dual-injection strategy, the authors plan to investigate the PM emissions production and optimize various engine control parameters.

5. Conclusions

This study compares the performance and emissions of a dual-injection strategy using a combination of fuels in a spark-ignition engine under certain experimental conditions with the injection and ignition timings selected for the engine speed of 1500 rpm. All the tests used gasoline in PFI and gasoline, ethanol or DMF in DI. For each of the three predetermined MAP_i (0.065, 0.08 and 0.095 MPa), the PFI mass fraction was reduced from 100% to 0%. The excess air ratio was controlled using the cross-over theory between the oxygen and carbon monoxide emissions concentrations. Normalized parameters were then used to study the effects of the combined fuelling technologies and fuels. Based on these experiments, the following conclusions can be drawn for the dual-injection strategy:

1. The cross-over theory of carbon monoxide and oxygen emissions concentration can be used to control the in-cylinder mixing ratio of oxygen content fuels with gasoline.
2. The IMEP increases with a decrease in the PFI mass fraction. Increasing DI fractions of ethanol or DMF contribute to higher performance gains, in terms of IMEP, than with gasoline.
3. Ethanol produces the highest indicated efficiency under all MAP_i. As the MAP_i increases, the impact on indicated efficiency is more positive compared to the 100% PFI case.
4. The combustion duration increases at all MAP_i when using increasing DI gasoline. However, at the highest MAP_i, the duration reduces by a maximum of at least 5% for the two biofuels.
5. The hydrocarbon (HC), oxides of nitrogen (NO_x) and carbon dioxide (CO_2) emissions are mostly reduced under the dual-injection strategy with increased gasoline and ethanol DI. For DMF, although the ISHC emissions reduce, the $ISCO_2$ and $ISNO_x$ emissions actually increase.
6. The preliminary combustion and emissions results show that the dual-injection strategy is advantageous at the lower PFI fractions and higher MAP_i.

In summary, the dual-injection strategy is a promising engine concept. It helps to utilize biofuels, reduce the dependency on fossil fuels, lower the engine-out emissions and improve the engine combustion, especially at the higher loads with less PFI mass fractions. Further work will be carried out using the dual-injection strategy to investigate the particulate matter emissions and to examine the extent of the improvements which can be obtained through spark timing optimization. The combustion and emissions performance of different gasoline–biofuel blends will also be compared between the DI strategy and the dual-injection equivalent.

Definitions, acronyms, abbreviations

AFR	air–fuel ratio
aTDC	after top dead centre
bTDC	before top dead centre
CAD	crank angle degree
CO	carbon monoxide
CO_2	carbon dioxide
DI	direct-injection
DMF	2,5-dimethylfuran
D50	50% by volume of 2,5-dimethylfuran in gasoline
ETH	ethanol
E50	50% by volume of ethanol in gasoline
HC	hydrocarbon
IMEP	indicated mean effective pressure
ISFCE	gasoline equivalent indicated specific fuel consumption
KL-MBT	knock-limited maximum brake torque
LHV	lower heating value
MAP	manifold absolute pressure
MBT	maximum brake torque
MFB	mass fraction burned
NO_x	nitrogen oxides
RPM	revolutions per minute
PFI	port fuel injection
TOL	toluene
ULG	gasoline
VVT	variable valve timing
WOT	wide-open throttle

Acknowledgments

This study was conducted in the Future Engines and Fuels laboratory at the University of Birmingham and was funded by the Engineering and Physical Sciences and Research Council (EPSRC) under the grant EP/F061692/1, the National Natural Science Foundation of China (Nos. 50821064, 50876085) and the China Scholarship Council (CSC). The authors would like to acknowledge the support from Jaguar Cars Ltd., Shell Global Solutions, UK and from various research assistants and technicians. Finally, the authors would like to acknowledge the support from their international collaborators at Tsinghua University.

References

[1] Heywood JB, Welling OZ. Trends in performance characteristics of modern automobile SI and diesel engines. SAE 2009-01-1892; 2009.
[2] DIRECTIVE 2009/28/EC. DIRECTIVE 2009/28/EC Official Journal of the European Union. 2009.
[3] US Ethanol Industry: the next inflection point. BCurtis Energies and Resource Group, 2007 year in review; 2008.
[4] Goldemberg J. The challenge of biofuels. Energy Environ Sci 2008;1:523–5.
[5] Alkidas AC, Tahry SHE. Contributors to the fuel economy advantage of DISI engines over PFI engines. SAE 2003-01-3101; 2003.
[6] Braisher M, Stone R, Price P. Particle number emissions from a range of european vehicles. SAE 2010-01-0786; 2010.
[7] Demirbas A. Progress and recent trends in biofuels. Prog Energy Combust Sci 2007;33:1–18.
[8] Demirbas A. Competitive liquid biofuels from biomass. Appl Energy 2011;88:17–28.
[9] Agarwal AK. Biofuels (alcohols and biodiesel) applications as fuels for internal combustion engines. Prog Energy Combust Sci 2007;33:233–71.
[10] Fatih Demirbas M. Biorefineries for biofuel upgrading: a critical review. Appl Energy 2009;86:S151–61.
[11] Mousdale DM. Bio-ethanol as a fuel: biotechnology, biochemical engineering and sustainable development. Boca Raton: CRC Press; 2008.
[12] Roman-Leshkov R, Barrett CJ, Liu ZY, Dumesic JA. Production of dimethylfuran for liquid fuels from biomass-derived carbohydrates. Nature 2007;447:982–6.

[13] Zhao H, Holladay JE, Brown H, Zhang ZC. Metal chlorides in ionic liquid solvents convert sugars to 5-hydroxymethylfurfural. Science 2007;316:1597–600.
[14] Binder JB, Raines RT. Simple chemical transformation of lignocellulosic biomass into furans for fuels and chemicals. J Am Chem Soc 2009;131:1979–85.
[15] Román-Leshkov Y, Barrett CJ, Liu ZY, Dumesic JA. Production of dimethylfuran for liquid fuels from biomass-derived carbohydrates. Nature 2007;447:982–5.
[16] Grela MA, Amorebieta VT, Colussi AJ. Very low pressure pyrolysis of furan, 2-methylfuran and 2,5-dimethylfuran. The stability of the furan ring. J Phys Chem 1985;89:38–41.
[17] Lifshitz A, Tamburu C, Shashua R. Thermal decomposition of 2,5-dimethylfuran. Experimental results and computer modeling. J Phys Chem A 1998;102:10655–70.
[18] Mascal M, Nikitin EB. Direct, high-yield conversion of cellulose into biofuel. Angew Chem Int Ed 2008;47:7924–6.
[19] Mousdale DM. Biofuels: biotechnology chemistry and sustainable development. U.K.: Taylor & Francis Group, CRC Press; 2008.
[20] Wu X, Huang Z, Yuan T, Zhang K, Wei L. Identification of combustion intermediates in a low-pressure premixed laminar 2,5-dimethylfuran/oxygen/argon flame with tunable synchrotron photoionization. Combust Flame 2009;156:1365–76.
[21] Wu X, Huang Z, Jin C, Wang X, Zheng B, Zhang Y, et al. Measurements of laminar burning velocities and Markstein lengths of 2,5-Dimethylfuran-air-diluent premixed flames. Energy Fuels 2009;23:4355–62.
[22] Wu X, Huang Z, Jin C, Wang X, Wei L. Laminar burning velocities and Markstein lengths of 2,5-dimethylfuran-air premixed flames at elevated temperatures. Combust Sci Technol 2011;183:220–37.
[23] Wu X, Huang Z, Wang X, Jin C, Tang C, Wei L, et al. Laminar burning velocities and flame instabilities of 2,5-dimethylfuran-air mixtures at elevated pressures. Combust Flame 2011;158:539–46.
[24] Zhong S, Daniel R, Xu H, Zhang J, Turner D, Wyszynski ML, et al. Combustion and emissions of 2,5-Dimethylfuran in a direct-injection spark-ignition engine. Energy Fuels 2010;24:2891–9.
[25] Daniel R, Tian G, Xu H, Wyszynski ML, Wu X, Huang Z. Effect of spark timing and load on a DISI engine fuelled with 25-dimethylfuran. Fuel 2011;90:449–58.
[26] Bromberg L, Cohn DR, Heywood JB. Water based systems for direct injection knock prevention in spark ignition engines. United States; 2010.
[27] Cohn DR, Bromberg L, Heywood JB. Fuel management system for variable ethanol octane enhancement of gasoline engines. In: Patent US, editor. United States: Massachusetts Institute of Technology (Cambridge, MA, US); 2010.
[28] Cohn DR, Bromberg L, Heywood JB. Direct injection ethanol boosted gasoline engines: biofuel leveraging for cost effective reduction of oil dependence and CO_2 emissions. Cambridge, MA 02139: Massachusetts Institute of Technology; 2005.
[29] Ikoma T, Abe S, Sonoda Y, Suzuki H, Suzuki Y, Basaki M. Development of V-6 3.5-liter engine adopting new direct injection system. SAE 2006-01-1259; 2006.
[30] Stein RA, House CJ, Leone TG. Optimal use of E85 in a turbocharged direct injection engine. SAE 2009-01-1490; 2009.
[31] Levine M. Ford's ''Bobcat'' Dual Fuel Engine 2009.
[32] Zhu G, Stuecken T, Schock H, Yang X, Hung DLS, Fedewa A. Combustion characteristics of a single-cylinder engine equipped with gasoline and ethanol dual-fuel systems. SAE 2008-01-1767; 2008.
[33] Zhu G, Hung D, Schock H. Combustion characteristics of a single-cylinder spark ignition gasoline and ethanol dual-fuelled engine. Proc Inst Mech Eng – Part D: J Automob Eng 2010;224:387–403.
[34] Stone R. Introduction to internal combustion engines. 3rd ed. Houndmills, Basingstoke [England]: SAE International and Macmillan Press; 1999.
[35] Heywood JB. Internal combustion engine fundamentals. New York: McGraw-Hill Book Company; 1988.
[36] Zhao F, Lai MC, Harrington DL. Automotive spark-ignited direct-injection gasoline engines. Prog Energy Combust Sci 1999;25:437–562.
[37] Tian G, Daniel R, Li H, Xu H, Shuai S, Richards P. Laminar burning velocities of 2,5-Dimethylfuran compared with ethanol and gasoline. Energy Fuels 2010;24:3898–905.
[38] Zervas E, Montagne X, Lahaye J. Emissions of regulated pollutants from a spark ignition engine. Influence of fuel and air/fuel equivalence ratio. Environ Sci Technol 2003;37:3232–8.
[39] Harrington JA, Shishu RC. A single-cylinder engine study of the effects of fuel type, fuel stoichiometry, and hydrogen-to-carbon ratio and Co, No, and Hc exhaust emissions. SAE 730476; 1973.